# Identification of Ductile Damage Parameters

Antonin Prantl[2], Jan Ruzicka[1], Miroslav Spaniel[1], Milos Moravec[1], Jan Dzugan[3], Pavel Konopík[3]

[1] Czech Technical University in Prague, Faculty of Mechanical Engineering,

[2]SKODA - JS a.s.

[3]Comtes FHT a.s.

*Abstract: This paper describes the calibration process for uncoupled material model of ductile damage by Johnson-Cook and Rice-Tracey that is implemented in FE package Abaqus. As the work was supported by the grant "Identification of ductile damage parameters for nuclear facilities", calibration was done for typical steel used in nuclear power plant industry. The project includes both design and realization of experiments, and application of experimental outputs in calibration process of material constants of mentioned ductile damage models. Calibration process of material model uses fifteen types of experimental specimens corresponding with literature. The result of the calibration process was verified through the comparison of FE simulation of each specimen with experimental response. As the material model describing ductile damage within the wide range of stress states was searched in this project, the model was tested on a several another specimens which exhibit higher stress concentration.*

*Keywords: Phenomenological material modeling, Ductile damage, Fracture Locus*

## 1. Introduction

Ductile damage is the process of metallic material damage in conditions of monotonic loading. Evolution of the damage follows plastic straining and ends by fracture of component. Problems of ductile damage play significant role in industry, for example in optimization of technological processes, evaluation of safety in automotive and aeronautic industry, analysis of steel civil structures etc. Complex material models of ductile fracture require calibration based on extensive experimental tests and their computational is costly as well. Thanks to progress of computational methods, namely FEA, such models can be nowadays used in engineering.

Phenomenological material models describing ductile damage in continuum mechanics mostly introduce extension of plasticity models. Two types of material models can be distinguished. Uncoupled models are separate plastic response and ductile damage and failure. Coupled models modify plastic response in dependence on damage evolution. Even though coupled models have huge potential, their complexity and calibration costs results into small extension in practice. Easier calibration process is an essential advantage of uncoupled material models, for which the calibration of plastic response and calibration of ductile damage can be separated. The calibration is distinctly easier if the uncoupled material model is used.

From the point of view of interpretation of real process inside material the ductile damage material models can be classified as either phenomenological models either micro-structural models.

Micro-structural models attempts to describe damage by natural way. Damage occurs on the basis of two different mechanisms. Initiation, growing and connecting of micro-cavities dominates in domains with tri-axial stress. Load carrying cross section is reduced during damage process and finally leads to failure. Based on representative volume with cavity some micromechanical continuum models were derived (Rice and Tracey, 1969, etc). However models based on this damage concept exhibit unrealistic response in domains at that pressure and shear stress are dominant. In this case material is damaged by localized shear strain in plane of maximal shear stress that holds an angle 45° with first principal plane. The phenomenological models do not have physical meaning and try best capture the behaving of real material on base of empirically designed relations. They are used for description of both of the two previously mentioned mechanisms. These models should be based on parameters having significant influence on ductile damage. The parameters are usually designed based on experience, intuition or are deduced from micromechanical continuum models. By the latter way the substantial influence of triaxiality stress was demonstrated. Formulation of failure criterion describing efficiently the process of damage is another crucial point of phenomenological models. Phenomenological models provide us with acceptable description of response in case of materials they was designed and calibrated for. On the other hand the experimental tests are costly and their portability to other materials is limited.

## 2. Ductile damage model

Material model discussed in this paper is based on both classical incremental model of plastic response with isotropic hardening and phenomenological concept of damage in continuum mechanic. This model supposes isotropy, and for description of stress state uses Von Mises stress $q$, stress triaxiality $\eta$ and Lode parameter $\xi$. These quantities are defined using second and third invariant of deviatoric stress

$$J_2 = \frac{1}{2}\left(S_1^2 + S_2^2 + S_3^2\right), \; J_3 = S_1 S_2 S_3 . \tag{1}$$

Principal deviatoric stresses $S_1$, $S_2$ and $S_3$ are principal values of stress deviator

$$\mathbf{S} = \boldsymbol{\sigma} + p\mathbf{I}, \; p = -\frac{1}{3} tr\left(\boldsymbol{\sigma}\right), \tag{2}$$

where $p$ is hydrostatic stress. Von Mises stress is defined as

$$q = \sqrt{3J_2} \; . \tag{3}$$

Stress triaxiality $\eta$ and Lode parameter $\xi$ can be expressed as

$$\eta = -\frac{p}{q}, \; \xi = \frac{27}{2}\frac{J_3}{q} . \tag{4}$$

The model of plastic response works with simple surface of plasticity that is based on Von Mises stress

$$q = \sigma_Y\left(\bar{\varepsilon}_{pl}\right), \tag{5}$$

associated flow rule and has the only one history dependent state parameter – accumulated intensity of plastic strain, resp. accumulated plastic strain

$$\bar{\varepsilon}_{pl} = \int_0^t \dot{\bar{\varepsilon}}_{pl} dt \ , \ \dot{\bar{\varepsilon}}_{pl} = \sqrt{\frac{2}{3}\dot{\boldsymbol{\varepsilon}}_{\mathbf{pl}} : \dot{\boldsymbol{\varepsilon}}_{\mathbf{pl}}} \ . \tag{6}$$

Dependence of $\sigma_Y\left(\bar{\varepsilon}_{pl}\right)$ is calibrated experimentally.

Failure criterion is based on phenomenological quantity damage $\omega$, that is defined as non-decreasing scalar parameter

$$\omega = \int_0^t \frac{\dot{\bar{\varepsilon}}_{pl} dt}{\bar{\varepsilon}_f\left(\eta, \xi\right)}, \tag{7}$$

that depends on loading history and can be understood as linear accumulation of incremental damage in process of monotonic loading. Fracture locus $\bar{\varepsilon}_f$ is function of stress triaxiality and Lode parameter and it has to be calibrated experimentally. Ductile fracture of material occurs as soon as critical damage value $\omega_{crit}$ is reached. The fracture locus has physical meaning of accumulated plastic strain at the instant of ductile damage initiation at the end of hypothetic monotonic loading with both triaxiality and Lode parameter constant. In such loading process the damage at failure reaches value $\omega_{crit} = 1$, so damage defined in (7) can be said to be normalized.

In this paper Johnson-Cook material model (Abaqus 6.12, 2012) was employed for description of ductile damage

$$\bar{\varepsilon}_f\left(\eta, \dot{\bar{\varepsilon}}_{pl}, \widehat{T}\right) = \left[d_1 + d_2 e^{-d_3\eta}\right]\left[1 + d_4 \ln\left(\frac{\dot{\bar{\varepsilon}}_{pl}}{\dot{\varepsilon}_0}\right)\right]\left(1 + d_5\widehat{T}\right), \tag{8}$$

where $d_1 ... d_5$ are failure parameters, $\dot{\varepsilon}_0$ is the reference strain rate, and $\widehat{T}$ is the dimensionless temperature. In this paper quasi-static loading at room temperature is supposed. Therefore only the first term (parameters $d_1, d_2, d_3$) of Johnson-Cook model is calibrated.

Exponential dependence of fracture locus on stress triaxiality also appears in material model Rice-Tracey (Rice, 1969) that is based on description of growing micro-cavities in basic material matrix. The Rice-Tracey model is defined

$$\bar{\varepsilon}_f\left(\eta\right) = C_{RT} e^{-\frac{3}{2}\eta}, \tag{9}$$

where $C_{RT}$ is failure parameter that has to be calibrated.

Bao and Wierzbicki (Bao, 2005) determined experimentally fracture locus in wide range of stress triaxiality and showed that the dependence of fracture locus on stress triaxiality need not be monotonic decreasing function. Xue and Wierzbicki (Wierzbicki, 2005) expanded the dependence of fracture strain on triaxiality by third invariant of stress tensor. This invariant was included in form of Lode parameter. Xue and Wierzbicki used elliptical function for description of dependence of fracture locus on Lode parameter. They defined symmetric function (fracture locus) that shows the same dependence of axisymmetric tension ( $\xi = 1$ ) and axisymmetric pressure ( $\xi = -1$ ). Further generalization is introduced in Bai-Wierzbicki model (Bai, 2007) that expects fracture locus generally asymmetric (Figure 1).

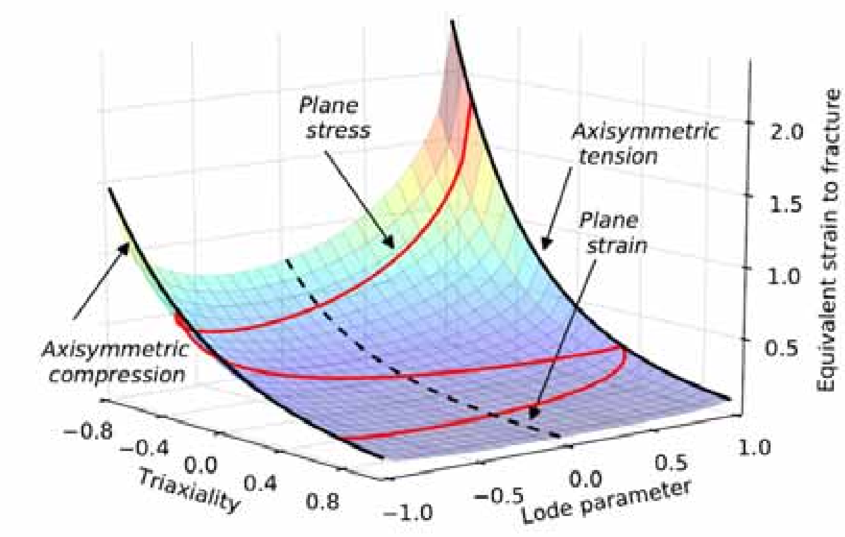


**Figure 1. Asymmetric fracture locus.**

The artificial degradation function described by parameter of degradation is implemented in Abaqus software and is created due to prevent stepped loss of stiffness in the whole element at the instant of failure criterion is reached. Difference between damage and degradation process is in dependence on fracture strain. The degradation is not included as material parameter and therefore it is not included in calibration process. Nevertheless the results of numerical simulation can be affected by choice of degradation. Since failure is indicated in the element of FE mesh the degradation manifesting itself as decrease of elastic modulus is started

$$E^{*} = (1 - D)E \tag{10}$$

After the critical value $D = 1$ is reached in element, it is removed form FE mesh. The damage process could be controlled by more ways in Abaqus. In this paper the description based on Hillerborg's fracture energy was used.

$$G_f = \int \mathrm{q}\, du_{pl} = \int Lq\; d\bar{\varepsilon}_{pl}\ . \tag{11}$$

Degradation process is defined as

$$D = \int \frac{Lq}{G_f} d\bar{\varepsilon}_{pl}\,, \tag{12}$$

where $L$ is characteristic size of element. As the Equation 12 shows, dependence of damage course on characteristic size of element $L$ is disadvantage of this approach. In area of expected damage the mesh with the same element size should be used. Material parameter $G_f$ must be recalculated for different mesh density. From Equation 11 the fracture energy $G_f$ can be expressed for any characteristic element length $L$ differing from $L_0$ using values of $G_{f0}$

$$\frac{G_f}{L} = \frac{G_{f0}}{L_0} = \int \mathrm{q}\; d\bar{\varepsilon}_{pl}\ \ ,\ G_f = \frac{G_{f0}}{L_0} L \tag{13}$$

Dependency of degradation development on mesh density can be removed by setting $G_f \rightarrow 0$. The phase of degradation is minimized and the full degradation of element occurs immediately after the critical damage value $\omega_{crit}$ is reached. All samples simulated in this paper have the same size of element edge (0.2 mm) in expected damage initiation. Small punch is exception. The element size of this type of specimen is 0.05 mm.

## 3. The methods of calibration

Several specimen types with different values of both stress triaxiality and Lode parameter at expected locations of ductile fracture should be used for successful calibration of material model.

Because in most cases the course of quantities ($\eta, \xi, \bar{\varepsilon}_{pl}$) during loading process can not be described using analytic formulas, the specimens have to be analyzed via FE. The calculated course of these quantities serves as input into calibration process. Experimental determination of fracture strain $\bar{\varepsilon}_f$ is essential. Mostly the critical extension $\Delta L_f$ at the instant of failure is determined from experimental data. Fracture strain $\bar{\varepsilon}_f$ in expected location of failure is then calculated using FE simulation. The critical extension could be determined for example via direct surface observation and first individual cracks detection. This approach is limited onto specimens at which the fracture starts form surface. Usually, critical extension is identified on base of sudden decrease of loading force in force-displacement record. It is possible to use the method of digital image correlation for direct evaluation of fracture strain in case of failure on the surface.

Two approaches are commonly cited to be used in calibration process of uncoupled ductile damage model. The first one is based on averaged values of stress triaxiality and Lode parameter (Bai, 2007) etc. Averaged values of stress triaxiality $\eta_{av}$, resp. Lode parameter $\xi_{av}$ are based on plastic strain weighted average

$$\eta_{av} = \frac{1}{\bar{\varepsilon}_f} \int_0^{\bar{\varepsilon}_f} \eta\left(\bar{\varepsilon}_{pl}\right) d\bar{\varepsilon}_{pl} \text{, resp. } \xi_{av} = \frac{1}{\bar{\varepsilon}_f} \int_0^{\bar{\varepsilon}_f} \xi\left(\bar{\varepsilon}_{pl}\right) d\bar{\varepsilon}_{pl} \,. \tag{14}$$

The point $\left[\eta_{av}, \xi_{av}, \bar{\varepsilon}_f\right]$ for each individual sample can be determined by this approach. Fracture locus $\bar{\varepsilon}_f(\eta, \xi)$ passes through this point. The main disadvantage of this approach is wide range of stress triaxiality and Lode parameter $\xi$ for some specimen types resulting into non-negligible error caused by averaging of these quantities. The point of minimum of target functional $F_{av}$

$$F_{av} = \sqrt[m]{\frac{1}{N} \sum_{i=1}^{N} \left| \bar{\varepsilon}_{f_i} - \bar{\varepsilon}_f\left(\eta_{av_i}, \xi_{av_i}\right) \right|^m} \tag{15}$$

is searched employing suitable optimization tools. This functional, at which $N$ means total number of calibrated specimens, $m$ expresses the rate of weighting of individual deviations, expresses total error of $\bar{\varepsilon}_f(\eta, \xi)$ in points $\left[\eta_{av_i}, \xi_{av_i}, \bar{\varepsilon}_{f_i}\right]$ corresponding with i-th specimen. More balanced deviation can be expected with growing value of $m$ ($m = 2$ corresponds with least squares method). Bai and Wierzbicki use modified target function $F_{av}^*$ in their work (Bai, 2007). Individual deviations are weighted by fracture strain.

$$F_{av}^* = \frac{1}{N} \sum_{i=1}^{N} \frac{1}{\bar{\varepsilon}_{f_i}} \left| \bar{\varepsilon}_{f_i} - \bar{\varepsilon}_f\left(\eta_{av_i}, \xi_{av_i}\right) \right| \tag{16}$$

Optional application of least squares enabling employment of linear regression is quality of this approach. Some material models can be modified so that the linear regression can be used partially.

The second approach defines target as deviation of damage $\omega_i$ integrated up to fracture strain $\omega_{crit} = 1$ for i-th specimen averaged over all specimens.

$$F_\omega = \sqrt[m]{\frac{1}{N}\sum_{i=1}^{N} \left| 1-\omega_i \right|^m} \ , \ \omega_i = \int_0^{\bar{\varepsilon}_{fi}} \frac{d\bar{\varepsilon}_{pl_i}}{\varepsilon_f(\eta_i,\xi_i)} \tag{17}$$

This approach eliminates averaging in Equation 13 however calibration costs are higher in comparison with the first approach and moreover existence of global minimum uncertainty is higher in this case. For this reasons fine tuning of parameters that was found using averaging quantities is preferred application. This approach was used for example in (Vaziri, 2010).

## 4. Experiments

Material calibration of ductile damage material model was carried out for steel typically used in nuclear industry. The portfolio of fifteen calibration specimen types for quasi-static loading was designed to calibrate fracture locus. Single specimens in space of stress triaxiality and Lode parameter are shown in Figure 2. It is based on averaged values of $\eta_{av}$ and $\xi_{av}$ at instant of expected fracture.

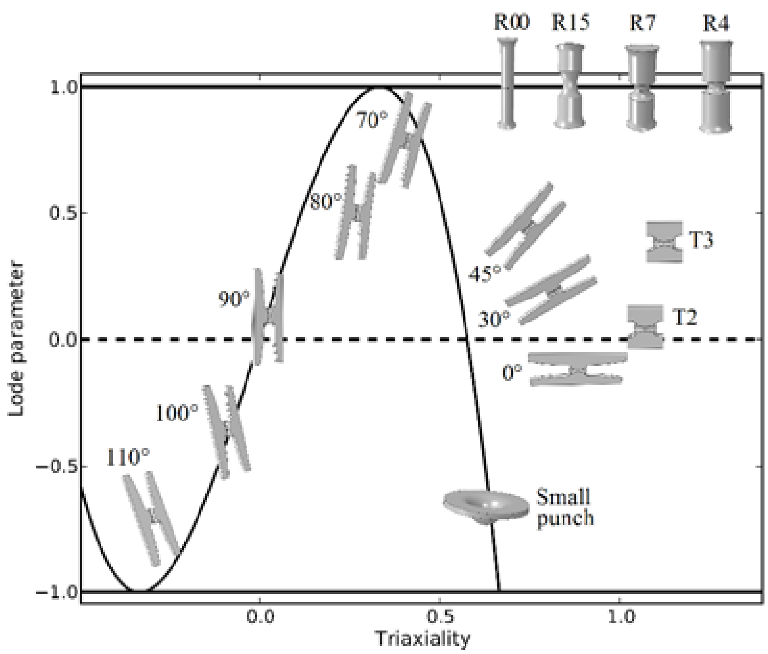

**Figure 2. The portfolio of calibration specimens.**

The substantial subset of calibration portfolio is based on special specimen with double curvature (butterfly) that was described in (Mohr, 2007). Essential advantage is possibility to cover wide range of stress triaxiality and normalized Lode angle with only one specimen geometry. Different stresses are caused by loading in different directions (tension: 0°, tension and share: 30° - 90°, compression and share: 100° - 130°). Another advantage is that damage initiation is always in centre of the specimen. The special testing device was developed to perform calibration tests using uniaxial loading machine. Figure 3 on the left shows example of device configuration. It was shown during the testing verification phase that the experimental data was distorted for the reason of friction in the guiding rods of the device. Therefore, simplified FE model of whole device (Figure 3 in the middle) is commonly used in numerical simulations of butterfly specimen. The friction coefficient was determined using try and error method to get correspondence with the experimental data. The disadvantage of this specimen type is shape complexity. The geometric inaccuracy may cause scattering between experimental data and FE simulations.

The basic configuration of the butterfly for angle position 0° was thanks to symmetry measured without device and undesirable friction effect was removed. FE models of specimens (Figure 3 on the right) use linear volume elements C3D8 with uniform edge size 0.2 mm in damaged area. In basic position 0° two modifications of the butterfly with double thickness (T2) and triple thickness (T3) were measured without device.

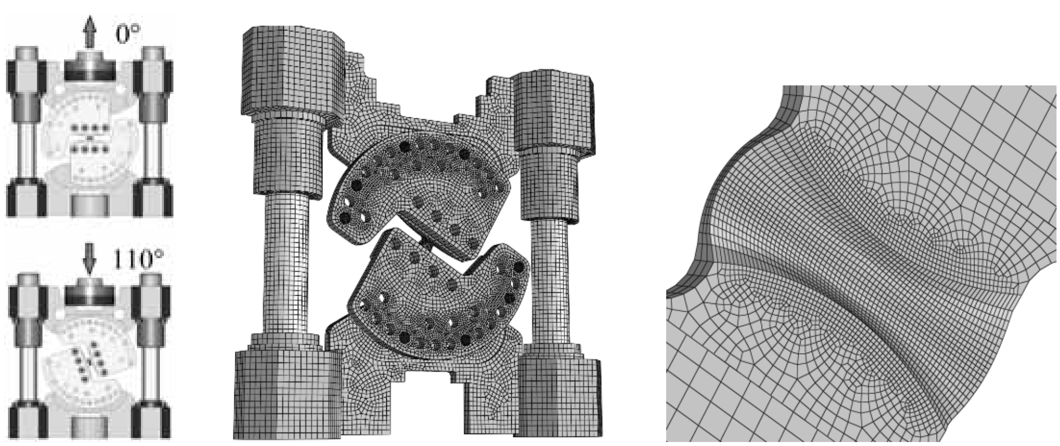


**Figure 3. The butterfly device FE model.**

The second subset of calibration specimens consists of notched round bars with different notches size (R∞, R15, R7 and R4). The specimen damage develops in conditions of constant value of

Lode parameter $\xi = 1$. Each of these specimens was designed so that the fracture occurs first in the centre of the specimen. The bilinear axisymmetric elements CAX4 with uniform size 0.2 mm in damage area was used (figure 4).

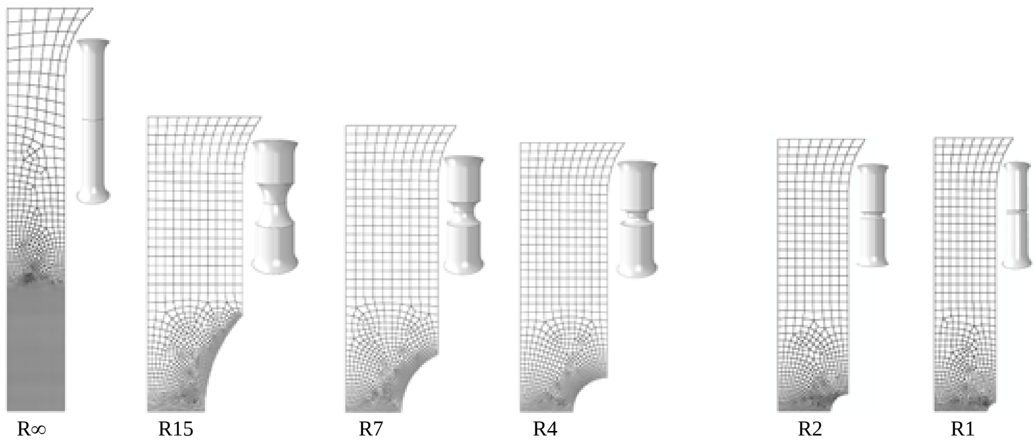


**Figure 4. Notched round bar specimens.**

The last calibration experiment is so called small punch test using miniature flat circular specimen through that the small steel ball is pushed. This experiment is used for verification of material properties of structures in operation from that small piece of material can be cut off without functionality loss. The specimen loading corresponds with biaxial tension. Disadvantage of this test is dependence on friction between ball and specimen. Friction coefficient that affects the place of damage initiation is uncertain, so we have chosen the best value within appropriate range. The bilinear axisymmetric elements CAX4 with global size 0.05 mm in damage area was used for FE simulation of the specimen (figure 5).

**Figure 5. FE model of small punch specimen**

## 5. Results of calibration process of damage material model

The calibration process was based on portfolio of fifteen different specimen types (Figure 2). The resultant fracture locus is shown in Figure 6. The figure introduces fracture strains of single specimens. Symbol associated with $i-\mathrm{th}$ specimen is plotted at position $\left[\eta_{av_i}, \xi_{av_i}, \bar{\varepsilon}_{f_i}\right]$.

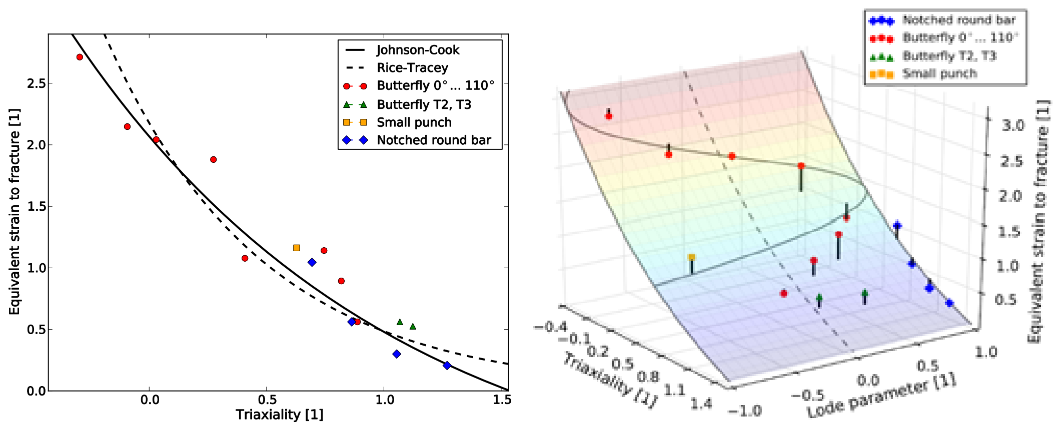


**Figure 6. Resultant Johnson-Cook and Rice-Tracey fracture locus.**

Fracture strain $\bar{\varepsilon}_f$ of this material showed to be independent on Lode parameter $\xi$. Therefore Johnson-Cook (the first term of Equation 8) and Rice-Tracey (Equation 9) material models are acceptable approximations for this kind of material. Figure 6 shows that Johnson-Cook fracture locus is non-positive for higher stress triaxiality by reason of negative parameter $d_1$. Therefore the fracture strain is supposed to be zero for $\eta > 1.5$.

The results of FE simulations for both used fracture locuses (Johnson-Cook and Rice-Tracey) are shown in subsequent figures. Response of Johnson-Cook material model is more close to experiments for most of specimens. It is possible to say that both models reach acceptable agreement with experimental data. Configuration with butterfly 120° was tested as well, but this specimen did not exhibit fracture until achievement of device limits which manifests itself as step in experimental loading curve in Figure 9.

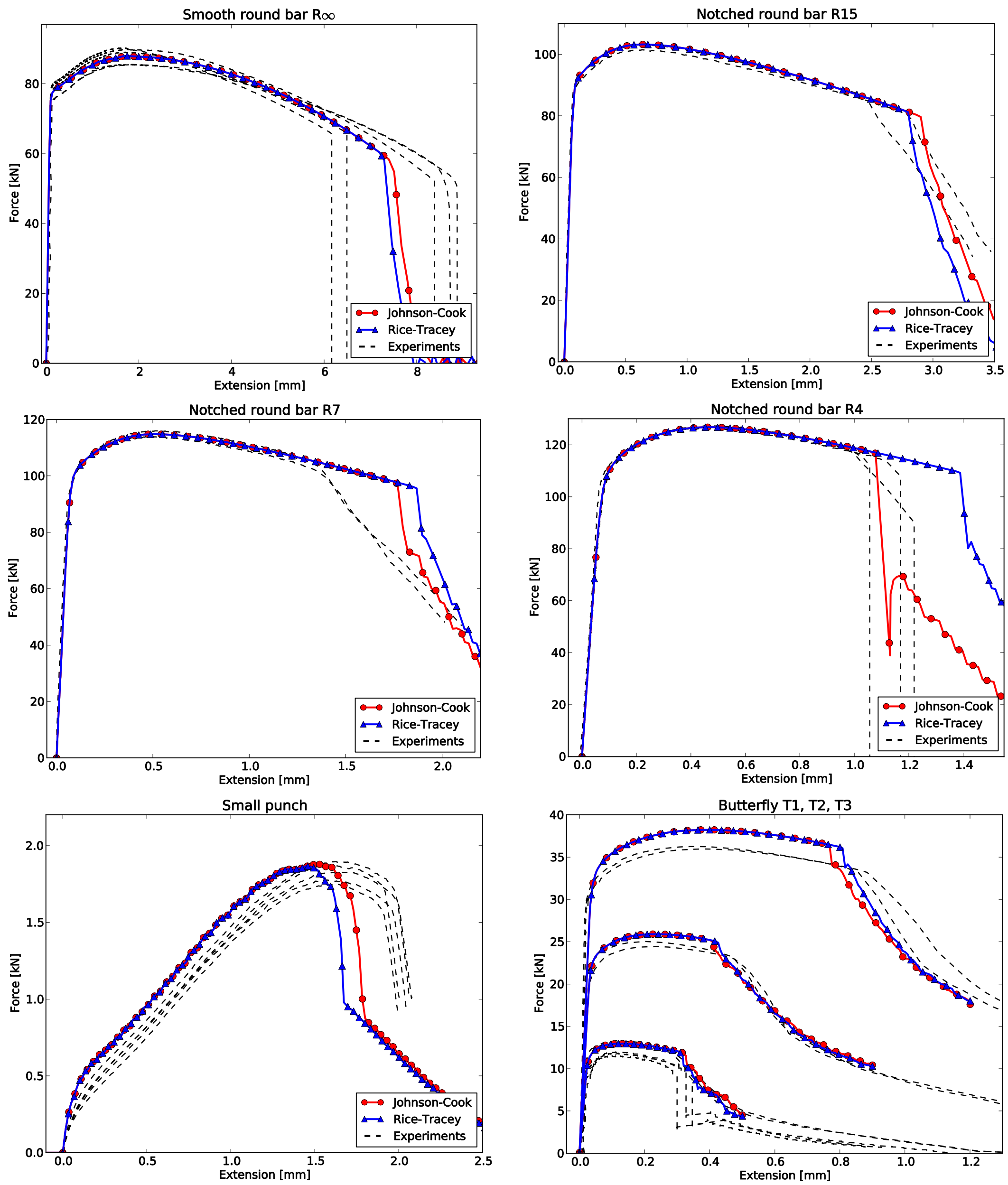


**Figure 7. The result of simulations with Johnson Cook and Rice Tracey model.**

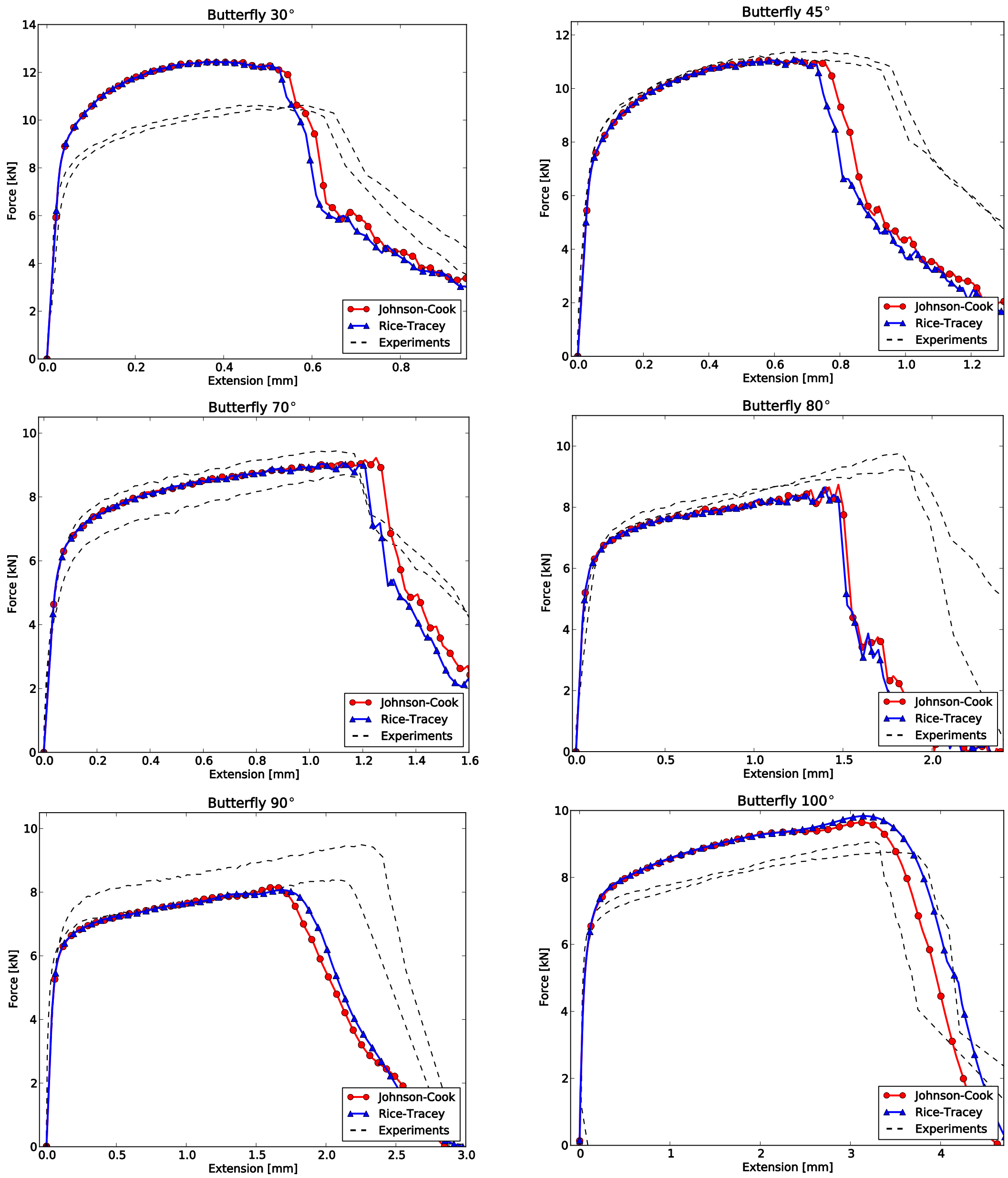


**Figure 8. The result of simulations with Johnson Cook and Rice Tracey model.**

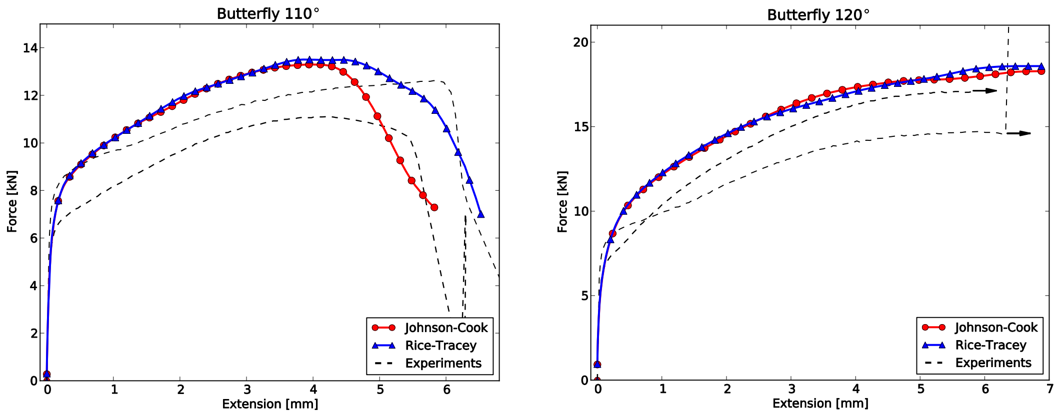


**Figure 9. The result of simulations with Johnson Cook and Rice Tracey model.**

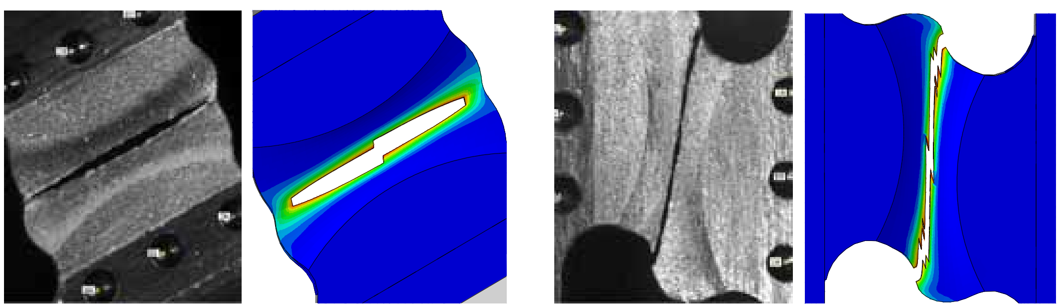

**Figure 10. Comparison of the fractured specimens butterfly 30° and butterfly 90°. Numerical simulations and experiments.**

## 6. The specimens with high local strain concentration

Calibration of material model that was performed using fifteen different specimens has proved ductile fracture of tested material dependency on stress triaxiality. Calibrated material model was tested on a few another specimen types with higher stress concentration. The series of notched round bars was expanded by new notched round bars R1 and R2 (Figure 4). Further specimen typically used in fracture mechanics – CT - without pre-crack was employed.

The comparison of experimental response of the specimens with FE simulations using Johnson-Cook and Rice-Tracey material model is presented in the Figure 11. The notched round bars with sharp notch showed acceptable correspondence between FE simulation and experimental data. Ductile fracture model exhibits poor results for CT when using Johnson-Cook ductile fracture model, while the result of Rice-Tracey model is acceptable (Figure 12). This is not in contradiction, because Rice-Tracey model was outlined on theoretical basis in the same form as Johnson Cook one with $d_1 = 1.5$. As the $d_1$ is calibrated parameter, Johnson-Cook model is in better correspondence in range of calibration tests, but it can be much worse outside it. The Figure also compares the final CT crack shape between experiment and FE (Rice-Tracey) simulation.

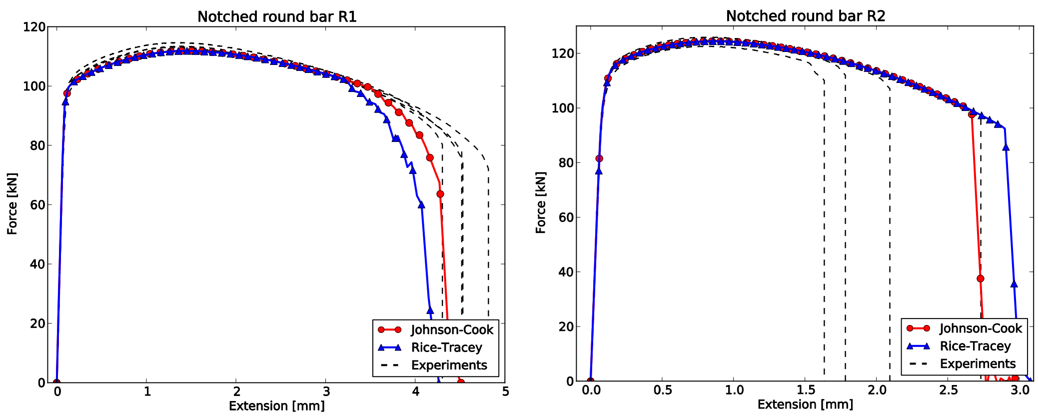


**Figure 11. The result of FE simulations of notched round bar R1 and R2 for Johnson Cook and Rice Tracey model.**

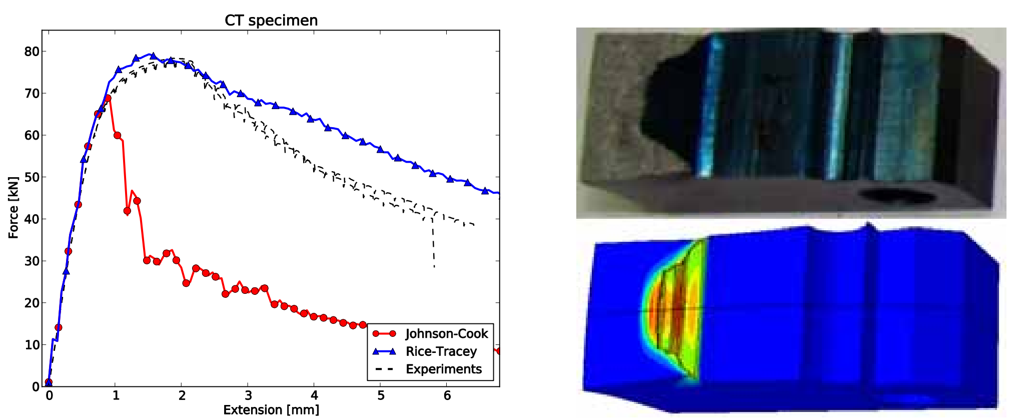


**Figure 12. The result of FE simulations of CT. Johnson Cook and Rice Tracey model. Final CT crack shape.**

## 7. Conclusions

Calibration of uncoupled phenomenological ductile fracture models (Johnson-Cook and Rice-Tracey) in FE software Abaqus was discussed. Fracture locus is expressed as function of stress triaxiality. Fracture strain was calculated on the base of the specimen extension at material failure. Portfolio of quasi-static calibrating tests was designed. Experiments on special specimen with double curvature (butterfly) which is loaded in different directions provided us with wide range of stress triaxiality and Lode parameter. For this type of the specimen special device allowing different loading angles had to be manufactured. In basic position 0° two modifications of butterfly with double and triple thickness were measured as well. Further tensile tests of notched round bars and small punch test were performed. Calibration of both ductile fracture models was carried out on steel typically used in nuclear industry. More accurate ductile fracture description in range of calibration experiments was reached using Johnson-Cook model. Both material models successfully describe ductile damage of calibration specimens that are commonly presented in the literature. In this paper the material models tests on specimens that showed local strain concentration was introduced. The notched round bars with sharp notch showed acceptable correspondence between FE simulation and experimental data. Ductile fracture of CT is poorly described when using Johnson-Cook model, but the result of Rice-Tracey model is well acceptable. We will focus on strain concentration in our further work.

## 8. References


1. Bai Y., Teng X., Wierzbicki T., “Derivation and application stress triaxiality formula for plane strain fracture testing”, Presented on the ASME conference, Austin, TX, June 3-7, 2007
2. Bao Y., Wierzbicki T., “On the cut-off value of negative triaxiality for fracture”, Engineering Fracture Mechanics, 72(7):1049-1069, 2005
3. Wierzbicki T., Xue L., “On the effect of the third invariant of the stress deviator on ductile fracture”, Technical report, Impact and Crashworthiness Laboratory, Massachusetts Institute of Technology, Cambridge, 2005
4. Rice JR., Tracey DM., “On the ductile enlargement of voids in triaxial stress fields”, Journal of the Mechanics and Physics of Solids, 17:201-217, 1969
5. Vaziri M.R., Salimi M., Mashayekhi M., “A new calibration method for ductile fracture models as chip separation criteria in machining”, Simulation Modelling Practice and Theory 18, 1286–1296, 2010
6. Mohr D., Henn S., “Calibration of Stress-triaxiality Dependent Crack Formation Criteria: A New Hybrid Experimental–Numerical Method“,Experimental Mechanics, 47(6), pp. 805-820
7. Abaqus 6.12 Online Documentation, 2012


## 9. Acknowledgment


This work was done within the work on the project “Ductile damage parameters identification for nuclear power plants - FR-TI2/279” sponsored by Ministry of Industry and Trade of The Czech Republic.